Hadron structure from lattice QCD

Ph. Hägler

Institut für Theoretische Physik T39, Physik-Department der TU München, 85747 Garching, Germany

Abstract. The last years have seen impressive progress in hadron structure calculations in dynamical lattice QCD. Form factors, moments of PDFs and GPDs, and many other important observables have been studied with increasing accuracy, giving access to fundamental physics questions, for example related to the distribution of charge and momentum in hadrons and the spin structure of the nucleon. We illustrate the recent achievements and remaining challenges by reviewing a small number of selected lattice results.

Keywords: lattice QCD, hadron structure
PACS: 12.38.Gc, 14.20.Dh

Introduction

The enormous efforts during the last decades in theoretical and experimental studies of elastic and deeply inelastic lepton-hadron scattering and related processes have provided detailed insights into many aspects of the structure of the nucleon. Complementary to these efforts, lattice QCD represents an excellent tool to investigate many fundamental hadron properties from first principles. Quantities which have been measured experimentally to a high precision, for example the axial vector coupling constant g_A or the nucleon magnetic moment μ, may be regarded as benchmark observables and indeed still pose a significant challenge for lattice calculations, see, e.g., [1, 2, 3]. In other cases, for example with respect to the energy momentum tensor and quark helicity flip (generalized) form factors, the lattice approach has distinct advantages over phenomenological studies, and provides already now great additional insight into the quark substructure of hadrons [4, 5, 6, 7].

As will become clear in the following sections, even the lattice hadron structure calculations at comparatively low pion masses of ≈ 300 MeV that have been reached in recent years still require highly non-trivial extrapolations to the physical point. Therefore solid predictions from chiral perturbation theory for the pion mass (and ideally also volume) dependence of the lattice data are of crucial importance.

Below, we first give a short overview of dynamical lattice calculations of the pion and the nucleon charge radius. This is followed by an update on moments of generalized parton distributions (GPDs) and the nucleon spin sum rule from the LHP collaboration. Finally, we present a first exploratory lattice study of transverse momentum dependent PDFs. For more detailed reviews of lattice hadron structure calculations, we refer to [8, 9, 10, 11].

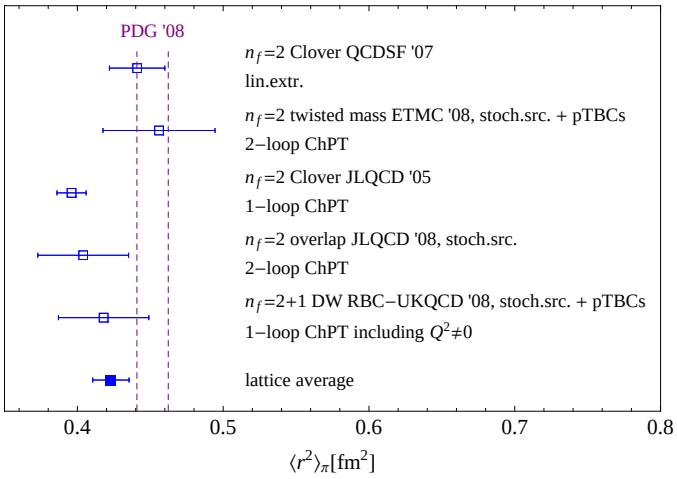

FIGURE 1. Overview of dynamical lattice QCD results for the chirally extrapolated pion mean square radius at the physical pion mass (references are provided in the text).

Hadron form factors and charge radii

The pion. Remarkable progress, mostly based on combinations of new methods and techniques, has been made in recent years with respect to lattice calculations of the pion electromagnetic form factor $F_\pi(Q^2)$, see, e.g., Refs. [12, 13, 14, 15, 16]. An illustrative example is the work by the RBC-UKQCD collaboration [16] that is based on $n_f = 2+1$ flavors of domain wall fermions, with a pion mass of $m_\pi = 330$ MeV, a lattice spacing of $a \approx 0.114$ fm, and a volume of $V \approx (2.74\text{ fm})^3$. In that study, the cost of the calculations was significantly reduced, and a high precision achieved, by using random wall sources instead of the conventional point sources for the computation of the quark propagators. Most importantly, very small, non-zero values of the momentum transfer in the range $Q^2 \approx 0.01,\ldots,0.04$ GeV^2 have been accessed by employing so-called partially twisted boundary conditions [17, 18]. It is remarkable that the smallest non-zero Q^2 reached in this lattice calculation is below the lowest Q^2 that could be so far accessed in experimental studies of $F_\pi(Q^2)$. Finally, from a chiral fit to the lattice data points using the original chiral perturbation theory result by Gasser and Leutwyler for $F_\pi(Q^2)$ [19], a pion charge radius of $\langle r_\pi^2\rangle = 0.418(31)$ fm^2 was found at the physical pion mass. This value is shown and compared to other recent lattice results and the experimental value in Fig. 1. Noting that the lattice values were obtained for a number of different lattice actions and chiral extrapolations, it is encouraging to see that they mostly agree within errors. It will be interesting to track down the origin of the slight discrepancy between the lattice average and experiment in future studies of the pion form factor.

The nucleon. During the recent years, a number of dynamical lattice calculations of the nucleon form factors were performed by different collaborations, with pion masses as low as ≈ 300 MeV [20, 21, 22, 23, 24, 25]. A fundamental observable derived from form factors is the mean square (ms) radius $\langle r^2\rangle \propto -(dF(Q^2)/dQ^2)_{Q^2=0}$. Figure 2 gives

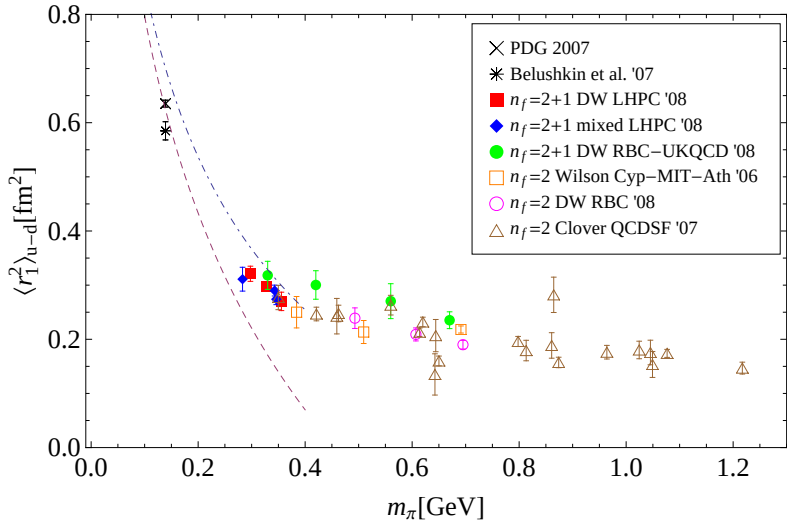

FIGURE 2. Overview of dynamical lattice QCD results for the isovector Dirac mean square radius (references are provided in the text). The dashed curve represents the leading 1-loop HBChPT prediction Bernard et al. [26], and the dotted-dashed curve the result obtained in the SSE Göckeler et al. [27].

on overview of results for the isovector Dirac ms radius $\langle r_1^2 \rangle_{u-d}$ as a function of the pion mass. Overall, the lattice data points obtained for the different actions and for $N_f = 2$ and $N_f = 2+1$ flavors are in good agreement within the statistical errors. Although the lattice values are slowly increasing towards smaller pion masses, they are still almost a factor of two below the phenomenological values, even at the lowest accessible lattice pion masses. Notwithstanding possible systematic uncertainties, this indicates that a strong chiral dynamics has to set in for $m_\pi < 300$ MeV, and ChPT calculations indeed predict that $\langle r_1^2 \rangle$ rises as $\ln(m_\pi)$ towards the chiral limit, as illustrated by the curves in Fig. 2. It is a major challenge to numerically demonstrate the presence of the predicted chiral singularity in lattice calculations at lower pion masses.

GPDs and the nucleon spin sum rule

One of the main motivations for the study of nucleon GPDs $H(x,\xi,t), E(x,\xi,t), \ldots$ (for reviews, see [28, 29, 30]) is their direct relation to the nucleon spin sum rule. As has already been shown in [31], the nucleon spin can be decomposed as

$$\frac{1}{2} = \frac{1}{2}\big(A(0)+B(0)\big) = \frac{1}{2}\big(\sum_q \langle x\rangle_q + \langle x\rangle_g + \sum_q B^q_{20}(0) + B^g_{20}(0)\big) \equiv \sum_q J_q + J_g\,, \qquad (1)$$

and is therefore, in addition to the momentum fractions $\langle x \rangle$ carried by the quarks and gluons, fully determined by the form factors $B_{q,g}(t)$ of the energy-momentum tensor at vanishing momentum transfer, $t = 0$ [1]. It turns out that the form factors $B_{q,g}(t)$ are

[1] $B_{q,g}(t=0)$ is also known as *anomalous gravitomagnetic moment* [32]

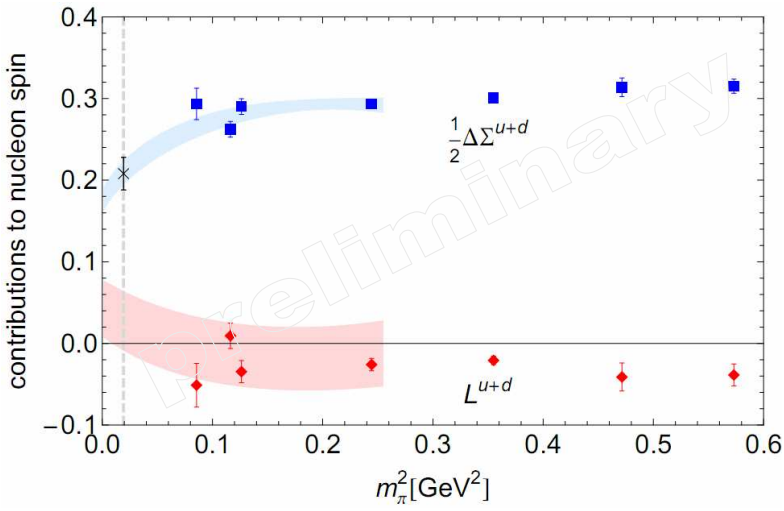

FIGURE 3. Contributions to the nucleon spin in the $\overline{\text{MS}}$ scheme at a scale of $\mu = 2$ GeV.

identical to the second x-moments of the GPDs $E^{q,g}(x,\xi,t)$ at $\xi = 0$,

$$B_{q,g}(t) = \int_{-1}^{1} dx x E^{q,g}(x,\xi=0,t)\,. \tag{2}$$

Furthermore, the total angular momentum of quarks can be naturally decomposed in a gauge-invariant manner in terms of quark spin and orbital angular momentum contributions, $J_q = \Delta\Sigma/2 + L_q$. Substantial progress has been made since the first lattice QCD calculations of moments of GPDs by the LHPC and QCDSF collaborations in 2003 [33, 34]. The so far most comprehensive lattice study of GPDs has been presented in [7] by LHPC based on a mixed action approach, which has been updated recently by inclusion of an additional ensemble at a lower pion mass of $m_\pi \approx 300$ MeV and by an increase in statistics by a factor of 8 [35]. Together with corresponding results for the quark spin fraction $\Delta\Sigma/2$, the lattice data for the form factors $A(t)$ and $B(t)$ was used to calculate the OAM carried by the quarks, displayed in Fig. 3 for $(u+d)$-quarks as a function of m_π^2. Results from a covariant chiral perturbation theory calculation [36] were employed to simultaneously extrapolate the energy momentum tensor form factors to $t = 0$ and the physical pion mass. This was combined with a heavy baryon ChPT fit of $\Delta\Sigma/2$ to obtain a chiral extrapolation of L^{u+d}, as illustrated by the error bands in Fig. 3. While the total quark spin turns out to be in very good agreement with results from HERMES [37], a very small OAM contribution of only $L^{u+d} \approx (5 \pm 5)\%$ is found at the physical pion mass. This is at first sight in striking disagreement with expectations from relativistic quark models, which predict that the quark OAM amounts to $\approx 30-40\%$ of the total nucleon spin. It has been noted, however, that the model calculations generically correspond to a low hadronic scale $\ll 1$ GeV, while the lattice scale is typically ≈ 2 GeV (with lattice results usually transformed to the $\overline{\text{MS}}$-scheme) [38, 39]. A naive, direct comparison of lattice and model results is therefore in general meaningless. Instead, one might attempt to employ QCD evolution to evolve the lattice values down to the lower model scale. This is displayed in Fig. 4 using NLO evolution. Indeed, the

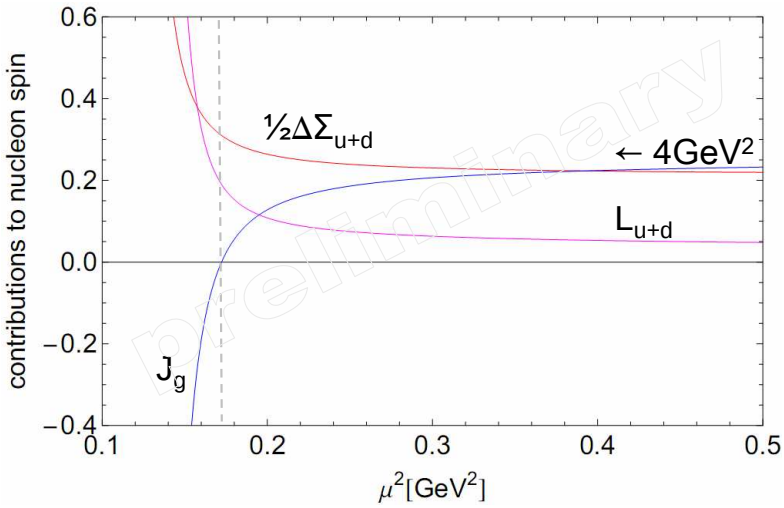

FIGURE 4. Evolution of contributions to the nucleon spin.

quark OAM increases substantial at lower scales, and a very good agreement with relativistic quark model results is found at the model scale, which has been fixed to the value at which the gluon contribution vanishes, $J_g = 0$ (indicated by the dashed vertical line in Fig. 4).

TMDs and the transverse nucleon spin structure

Another important class of observables is given by the so-called transverse momentum dependent parton distribution functions (TMDs). They encode fundamental information about hadron structure that is mostly complementary to the physics content of PDFs and GPDs. TMDs are generically denoted by $[f,g,h](x,k_\perp^2)$, and depend, in addition to the longitudinal momentum fraction x, also on the intrinsic transverse momentum $k_\perp$ carried by the partons. They have in general a probability density interpretation (for issues related to the high-$k_\perp$ behavior and the integrability of TMDs we refer to [40]), similar to the generalized parton distributions (GPDs) in impact parameter ($b_\perp$)-space [41]. It is interesting to note that although the transverse momentum, $k_\perp$, and the coordinate, $b_\perp$, are *not* Fourier-conjugated variables, a number of *approximate* relations between TMDs and GPDs have been established and conjectured [42, 43, 44]. TMDs play a central role in the phenomenology of semi-inclusive deep inelastic scattering (SIDIS) and the Drell-Yan-process, where correlations between the intrinsic transverse momenta of the partons, the hadron momenta, and their spins lead to a variety of interesting asymmetries. A lot of attention has been attracted by the Sivers- and Collins-effect [45, 46], which give rise to single spin azimuthal asymmetries in SIDIS, and which have already been studied experimentally at HERMES, COMPASS and BELLE [47, 48, 49].

Recently, we have performed a first lattice QCD study of $k_\perp$-distributions [50, 51, 52]. The calculations were based on (nucleon matrix elements of) manifestly non-local, gauge invariant quark operators, giving access to a number of invariant amplitudes.

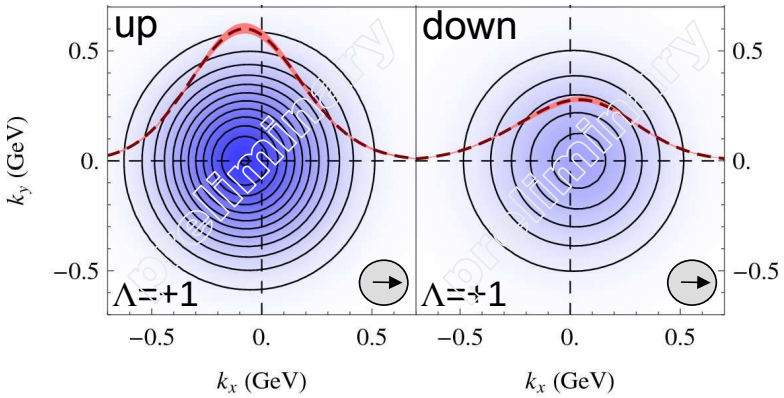

FIGURE 5. Transverse momentum densities of quarks in the nucleon.

The numerical lattice results for these amplitudes can in turn be parametrized and then Fourier-transformed to obtain the $k_\perp$-distributions. A very useful interpretation of the various $k_\perp$-dependent PDFs can be given in form of quark densities in the transverse momentum plane. For transversely polarized quarks with spin $s_\perp$ in a longitudinally polarized nucleon with helicity Λ, the density is given by [43]

$$\rho_T = \frac{1}{2}\left(f_1 + s_\perp \cdot S_\perp h_1 + \left[\frac{s_j \varepsilon_{ji} k_i}{m_N} h_1^\perp \right] + \frac{s_j (2k_j k_i - k_\perp^2 \delta_{ji}) S_i}{2m_N^2} h_{1T}^\perp + \Lambda \frac{k_\perp \cdot s_\perp}{m_N} h_{1L}^\perp \right), \quad (3)$$

similar to a multipole-expansion, with monopole terms $\propto f_1, h_1$, dipole structures $\propto h_1^\perp, h_{1L}^\perp$, and a quadrupole term $\propto h_{1T}^\perp$. Note that all TMDs in Eq. 3 depend on x and $k_\perp^2$, and that the term in square brackets is absent for our choice of non-local lattice operators. The lattice results for the lowest x-moment of the density $\rho_T(x, k_\perp)$ are illustrated in Fig. 5 for up- and down-quarks on the left and the right, respectively, with $s_\perp = (1,0)$ and $\Lambda = +1$. Due to the non-zero results for the distributions $h_{1L}^{\perp,u} < 0$, $h_{1L}^{\perp,d} > 0$ in particular, we observe a significant correlation between the quark transverse spin and intrinsic transverse momentum, leading to clearly visible dipole deformations in opposite directions for up- and for down-quarks in Fig. 5 . Since the distribution $h_{1L}^\perp$ has, in contrast to nearly all others TMDs, no analog in the framework of GPDs due to time reversal symmetry, the deformations may be seen as a genuine effect of intrinsic $k_\perp$ of quarks in the nucleon. We note that it is very illustrative to contrast the $k_\perp$-densities in Fig. 5 with lattice results for impact-parameter ($b_\perp$-) densities based on moments of GPDs, presented in [5] for the nucleon, and in [6] for the pion.

ACKNOWLEDGMENTS

It is a pleasure to thank M. Altenbuchinger, B. Musch and W. Weise from the theory group T39 at the TU München, and the colleagues from the LHPC and the QCDSF collaborations. I gratefully acknowledge the support by the Emmy-Noether program and the cluster of excellence “Origin and Structure of the Universe” of the DFG.

REFERENCES

1. R. G. Edwards, et al., *Phys. Rev. Lett.* **96**, 052001 (2006), hep-lat/0510062.
2. A. A. Khan, et al., *Phys. Rev.* **D74**, 094508 (2006), hep-lat/0603028.
3. S. N. Syritsyn, et al. (2009), 0907.4194.
4. M. Göckeler, et al., *Phys. Lett.* **B627**, 113–123 (2005), hep-lat/0507001.
5. M. Göckeler, et al., *Phys. Rev. Lett.* **98**, 222001 (2007), hep-lat/0612032.
6. D. Brömmel, et al., *Phys. Rev. Lett.* **101**, 122001 (2008), 0708.2249.
7. P. Hägler, et al., *Phys. Rev.* **D77**, 094502 (2008), 0705.4295.
8. K. Orginos, *PoS* **LAT2006**, 018 (2006).
9. P. Hägler, *PoS* **LAT2007**, 013 (2007), 0711.0819.
10. J. M. Zanotti, *PoS* **LAT2008**, 007 (2008), 0812.3845.
11. A. Schäfer, *Nucl. Phys.* **A805**, 230–239 (2008).
12. S. Hashimoto, et al., *PoS* **LAT2005**, 336 (2006), hep-lat/0510085.
13. D. Brömmel, et al., *Eur. Phys. J.* **C51**, 335–345 (2007), hep-lat/0608021.
14. R. Frezzotti, V. Lubicz, and S. Simula (2008), 0812.4042.
15. JLQCD, et al. (2008), 0810.2590.
16. P. A. Boyle, et al., *JHEP* **07**, 112 (2008), 0804.3971.
17. C. T. Sachrajda, and G. Villadoro, *Phys. Lett.* **B609**, 73–85 (2005), hep-lat/0411033.
18. P. F. Bedaque, and J.-W. Chen, *Phys. Lett.* **B616**, 208–214 (2005), hep-lat/0412023.
19. J. Gasser, and H. Leutwyler, *Ann. Phys.* **158**, 142 (1984).
20. C. Alexandrou, G. Koutsou, J. W. Negele, and A. Tsapalis, *Phys. Rev.* **D74**, 034508 (2006), hep-lat/0605017.
21. M. Göckeler, et al. (2007), 0709.3370.
22. S. Syritsyn, et al., *PoS* **LAT2008**, 169 (2008).
23. J. D. Bratt, et al., *PoS* **LATTICE2008**, 141 (2008), 0810.1933.
24. H.-W. Lin, et al., *Phys. Rev.* **D78**, 014505 (2008), 0802.0863.
25. S. Ohta, and T. Yamazaki (2008), 0810.0045.
26. V. Bernard, N. Kaiser, J. Kambor, and U. G. Meissner, *Nucl. Phys.* **B388**, 315–345 (1992).
27. M. Göckeler, et al., *Phys. Rev.* **D71**, 034508 (2005), hep-lat/0303019.
28. K. Goeke, M. V. Polyakov, and M. Vanderhaeghen, *Prog. Part. Nucl. Phys.* **47**, 401–515 (2001), hep-ph/0106012.
29. M. Diehl, *Phys. Rept.* **388**, 41–277 (2003), hep-ph/0307382.
30. A. V. Belitsky, and A. V. Radyushkin, *Phys. Rept.* **418**, 1–387 (2005), hep-ph/0504030.
31. X.-D. Ji, *Phys. Rev. Lett.* **78**, 610–613 (1997), hep-ph/9603249.
32. O. V. Teryaev (1999), hep-ph/9904376.
33. P. Hägler, et al., *Phys. Rev.* **D68**, 034505 (2003), hep-lat/0304018.
34. M. Göckeler, et al., *Phys. Rev. Lett.* **92**, 042002 (2004), hep-ph/0304249.
35. LHPC, in preparation (2009).
36. M. Dorati, T. A. Gail, and T. R. Hemmert, *Nucl. Phys.* **A798**, 96–131 (2008), nucl-th/0703073.
37. A. Airapetian, et al., *Phys. Rev.* **D75**, 012007 (2007).
38. M. Wakamatsu, and Y. Nakakoji, *Phys. Rev.* **D77**, 074011 (2008), 0712.2079.
39. A. W. Thomas, *Phys. Rev. Lett.* **101**, 102003 (2008), 0803.2775.
40. A. Bacchetta, D. Boer, M. Diehl, and P. J. Mulders, *JHEP* **08**, 023 (2008), 0803.0227.
41. M. Burkardt, *Phys. Rev.* **D62**, 071503 (2000), hep-ph/0005108.
42. M. Burkardt, *Phys. Rev.* **D66**, 114005 (2002), hep-ph/0209179.
43. M. Diehl, and P. Hägler, *Eur. Phys. J.* **C44**, 87–101 (2005), hep-ph/0504175.
44. S. Meissner, A. Metz, and K. Goeke, *Phys. Rev.* **D76**, 034002 (2007), hep-ph/0703176.
45. D. W. Sivers, *Phys. Rev.* **D41**, 83 (1990).
46. J. C. Collins, *Nucl. Phys.* **B396**, 161–182 (1993).
47. A. Airapetian, et al., *Phys. Rev. Lett.* **94**, 012002 (2005), hep-ex/0408013.
48. V. Y. Alexakhin, et al., *Phys. Rev. Lett.* **94**, 202002 (2005), hep-ex/0503002.
49. K. Abe, et al., *Phys. Rev. Lett.* **96**, 232002 (2006), hep-ex/0507063.
50. B. U. Musch, et al. (2008), 0811.1536.
51. B. Musch, Ph.D. thesis, TU Munich (2009).
52. P. Hägler, B. Musch, J. Negele, and A. Schäfer, to be published (2009).